The role of desmoglein-2 in kidney disease

Tong Xu[1,2,10], Lea Herkens[1,10], Ting Jia[1,3], Barbara M. Klinkhammer[1], Sebastian Kant[4], Claudia A. Krusche[4], Eva M. Buhl[5], Sikander Hayat[6], Jürgen Floege[7], Pavel Strnad[8], Rafael Kramann[6,7,9], Sonja Djudjaj[1,11] and Peter Boor[1,5,7,11]

[1]*Institute of Pathology, RWTH Aachen University, Aachen, Germany;* [2]*Department of Urology, the First Affiliated Hospital of Airforce Medical University, Xi'an, China;* [3]*Department of Nephrology, the Second Affiliated Hospital of Xi'an Jiaotong University, Xi'an, China;* [4]*Institute of Molecular and Cellular Anatomy, RWTH Aachen University, Aachen, Germany;* [5]*Electron Microscopy Facility, RWTH Aachen University, Aachen, Germany;* [6]*Institute of Experimental Medicine and Systems Biology, RWTH Aachen University, Aachen, Germany;* [7]*Division of Nephrology and Clinical Immunology, RWTH Aachen University, Aachen, Germany;* [8]*Department of Medicine III, Gastroenterology, Metabolic Diseases and Intensive Care, RWTH Aachen University, Aachen, Germany; and* [9]*Department of Internal Medicine, Nephrology and Transplantation, Erasmus Medical Center, Rotterdam, the Netherlands*

OPEN

Desmosomes are multi-protein cell-cell adhesion structures supporting cell stability and mechanical stress resilience of tissues, best described in skin and heart. The kidney is exposed to various mechanical stimuli and stress, yet little is known about kidney desmosomes. In healthy kidneys, we found desmosomal proteins located at the apical-junctional complex in tubular epithelial cells. In four different animal models and patient biopsies with various kidney diseases, desmosomal components were significantly upregulated and partly miss-localized outside of the apical-junctional complexes along the whole lateral tubular epithelial cell membrane. The most upregulated component was desmoglein-2 (Dsg2). Mice with constitutive tubular epithelial cell-specific deletion of *Dsg2* developed normally, and other desmosomal components were not altered in these mice. When challenged with different types of tubular epithelial cell injury (unilateral ureteral obstruction, ischemia-reperfusion, and 2,8-dihydroxyadenine crystal nephropathy), we found increased tubular epithelial cell apoptosis, proliferation, tubular atrophy, and inflammation compared to wild-type mice in all models and time points. *In vitro*, silencing *DSG2* via siRNA weakened cell-cell adhesion in HK-2 cells and increased cell death. Thus, our data show a prominent upregulation of desmosomal components in tubular cells across species and diseases and suggest a protective role of Dsg2 against various injurious stimuli.

Kidney International (2024) ■, ■–■; https://doi.org/10.1016/j.kint.2024.01.037

Correspondence: *Peter Boor, Institute of Pathology, RWTH Aachen University Hospital, Pauwelsstrasse 30, 52074 Aachen, Germany. E-mail: pboor@ukaachen.de*

[10]TX and LH shared first authorship.

[11]SD and PB shared last authorship.

Received 8 November 2022; revised 7 December 2023; accepted 9 January 2024

KEYWORDS: desmosome; kidney injury; kidney tubular epithelial cells; mechanical stress

Translational Statement

We have found a significant upregulation of desmosomal components in kidney tubular cells in various preclinical disease models and patient biopsies, the most prominent being desmoglein-2 (Dsg2). In genetically modified animals with tubular cell–specific deletion of *Dsg2*, we found that *Dsg2* was dispensable for normal kidney development, but its deletion aggravated kidney tubular injury and inflammation in various disease models and weakened cell-cell connection. Our data support the role of mechanical stress in the pathogenesis of kidney diseases and uncover a novel molecular mechanism protecting tubular cells from injury.

Kidney tubular epithelial cells (TECs) represent the largest cell population in the kidneys and are essential for normal kidney function. TECs are known to react sensitively to many injurious stimuli, such as hypoxia, crystals, toxins, or inflammation. Acute TEC injury is a common pathologic finding in kidney biopsies and the main pathologic correlate of acute kidney injury.[1]

Desmosomes are cell-cell adhesion structures that serve as anchors for the cytoplasmic intermediate filament cytoskeleton, providing tissues with mechanical coherence and stability.[2,3] Desmosomes are multiprotein complexes comprising the cytoskeleton-associated protein desmoplakin (Dsp), which directly binds to the cytoplasmic intermediate filaments in the inner dense desmosomal plaque. This binding is further stabilized by the armadillo protein family, which consists of plakoglobin (Pg) and plakophilin (Pkp1–4). Pg and Pkp bind to 2 intercellular cadherin protein families, that is, desmoglein (Dsg1–4) and desmocollin (Dsc1–3), which bridge the extracellular space and interact with each other to

mediate the connection to adjacent cells. Dsg2 and Dsc2 are the most abundant members of desmosomal cadherins in simple epithelia.[4–7]

The role of desmosome is best described in the skin and the heart, that is, organs constantly exposed to mechanical stress. Studies showed that autoantibodies against Dsg1 and Dsg3 lead to pemphigus vulgaris and pemphigus foliaceous in the skin, severe blistering diseases of the skin, and the mucosa.[8,9] Mutations in *DSG2*, *PKP2*, or *DSP* result in arrhythmogenic right ventricular cardiomyopathy possibly due to impaired cell-cell adhesion. Some desmosomal components, for example, Dsg2, were also described to be involved in regulating proliferation, apoptosis, migration, and inflammation.[10–15]

Previously we have shown that keratins, the intermediate filaments of the TEC cytoskeleton that are anchored to desmosomes, were prominently upregulated in stress situations in TECs in a wide range of kidney diseases.[16] Furthermore, mislocalization of desmosomal proteins was noted in autosomal dominant polycystic kidney disease.[17,18] The desmosomal proteins Dsp, Dsg1, and Dsc2 were found to be expressed in TECs in the developing kidneys of humans and mice.[19] However, no data are available on the expression, regulation, and functional role of desmosomes and desmosomal components in other kidney diseases.

Here we comprehensively characterized the expression and regulation of different desmosomal components in healthy kidneys and different kidney diseases in preclinical models and patient biopsies and analyzed the functional consequences of tubular cell deletion of Dsg2 in transgenic mice.

METHODS

Study design and ethics

Human kidney samples were collected from biopsy and resection specimens at the Institute of Pathology of the University Clinic RWTH Aachen. All samples were handled anonymously, and the study was approved by the local review board (EK244/14 and EK042/17) and in line with the Declaration of Helsinki. In total, 33 patient kidney samples were included in the study, involving healthy human kidneys (n = 5), renovascular disease (n = 2), pyelonephritis (n = 5), hydronephrosis/nephrolithiasis (n = 5), acquired cystic kidney disease (ACKD) (n = 6), autosomal dominant polycystic kidney disease (n = 5), and T-cell–mediated rejection injury (n = 5). Patient characteristics are shown in Table 1 and Supplementary Figure S1.

Animal experiments. In total, 33 C57Bl/6N wild-type male mice, 28 *Pax8-Cre::Dsg2*$^{flox/flox}$ male mice, 23 *Pax8-Cre::Dsg2*$^{flox/flox}$ female mice, 43 wild-type male littermates, and 26 wild-type female littermates (all animals aged 10–14 weeks, except the mice or the aging experiment) were employed and induced to the below-mentioned disease models. The animals were kept in animal facility of the University Hospital RWTH Aachen with constant temperature, humidity, and 12-hour light-dark cycles. Tap water and standard chow were freely accessible. Each mouse had an individual ID number, and detailed records were kept of its rearing, grouping, surgical records, sampling, and data analysis. Mice were randomly assigned to each group and excluded if there were any problems during surgery, and no damage was visible in the periodic acid–Schiff staining. The sample size was determined based on the number of experimental groups and different analysis time points. Animals of the same sex (male/female), age, and body weight were divided into groups for comparison. The operation was performed by the same experienced member. In this way, experimental error is reduced. Every effort was made to minimize animal suffering, and all animal experiments were approved by the local government authorities (Landesamt für Natur, Umwelt und Verbraucherschutz Nordrhein-Westfalen).

Table1 | Patient characteristics

Patients' profile	Healthy group (n = 5)	Disease group (n = 28)	*P* value
Age, yr, mean ± SD	47.4 ± 27.2	52.5 ± 14.8	NS
Gender, %, male	100	68	NS
Urea, mg/dl, mean ± SD	30.4 ± 9.5	81.4 ± 46.9	<0.05
Serum creatinine, mg/dl, mean ± SD	0.8 ± 0.4	5.5 ± 4.8	<0.05
eGFR, mean ± SD	67.9 ± 15.3	33.8 ± 33.6	NS
BMI, mean ± SD	21.8 ± 4.4	29.6 ± 11.9	NS

BMI, body mass index; eGFR, estimated glomerular filtration rate; NS, not significant.

Unilateral ureteral obstruction model

In the unilateral ureteral obstruction (UUO) model, the left ureter was ligated by electrocauterization as described previously.[16] As controls (sham, n = 3), mice underwent the same surgery procedure except for the ureter ligation step. The following time points were performed in male C57Bl/6N wild-type mice: UUO 12 hours (n = 4), day 1 (n = 4), day 5 (n = 6), day 7 (n = 5), day 14 (n = 6), and day 21 (n = 4). In a second approach, UUO day 5 and day 10 were performed in male *Pax8-Cre::Dsg2*$^{flox/flox}$ (day 5: n = 9; day 10: n = 8) and wild-type littermates (day 5: n = 8, day 10: n = 16).

Ischemia-reperfusion model

We used female *Pax8-Cre::Dsg2*$^{flox/flox}$ (n = 8) and wild-type littermates (n = 13) for this model. Ischemia-reperfusion (I/R) was performed by clamping the left renal artery with a micro-serrefine clip for 35 minutes as previously described.[20] A heating blanket was used during the surgical procedure to keep a constant temperature of 37 °C. Kidneys were harvested on day 21 after the surgery.

Bilateral I/R model

Bilateral I/R was performed in male *Pax8-Cre::Dsg2*$^{flox/flox}$ (n = 8) and wild-type littermates (n = 16) by clamping the left and right renal artery with a micro-serrefine clip for 25 minutes. During the surgical procedure, a constant temperature of 37 °C was kept, and the mice were sacrificed after 24 hours. Urine was collected before the operation and 6 hours before the mice were sacrificed.

2,8-Dihydroxyadenine nephropathy model (adenine)

This model was performed in female *Pax8-Cre::Dsg2*$^{flox/flox}$ (n = 10) and wild-type littermates (n = 9) and induced by administration of an adenine-rich diet (supplemented with 0.2% adenine). All mice had free access to adenine chow and water *ad libitum* as previously described.[21] The mice were sacrificed 14 days after starting the adenine diet, and kidney, urine, and serum were collected.

Other methods

All other methods used in this study can be found in the Supplementary Methods, that is, *in vitro* cell culture experiments

(Supplementary Tables S1 and S2), histology, immunohistochemistry (Supplementary Table S3) and immunofluorescence, RNA extraction and analysis (Supplementary Table S4), Western blot analysis (Supplementary Table S5), public array analysis (Supplementary Table S6), digital data analysis, and single-cell RNA sequencing (scRNA-seq).

Statistical analysis

The sample size of each group included at least 3 animals. All statistical analyses were performed using GraphPad Prism 8.3.0 (GraphPad). Data are presented as mean ± SD. The 2-tailed unpaired Student t test was applied for the comparison of 2 groups. One-way analysis of variance with Turkey correction was used for the comparison of multiple groups. Statistical significance was defined as $P < 0.05$. The adjusted P value in the publicly available datasets was provided by the online datasets. The acceptable error rate was 5%.

RESULTS

Expression of desmosomal proteins in kidneys

First, we confirmed the localization of the desmosomes in healthy murine and human kidney TECs by electron microscopy, showing that the typical desmosomal structures were predominantly localized at the apical-junction complexes directly beneath tight and adherens junctions (Figure 1a and b). In kidney diseases, we observed an increased number of desmosomes in both mice and humans (Figure 1c and d). The analysis of scRNA-seq data from human kidneys[22] confirmed the expression of mRNA of desmosomal components mainly in TECs, with particularly strong expression of *DSG2* (Supplementary Figure S2).

In healthy mice, the expression of nearly all members of desmosomal proteins was confined to TECs, localized at the apical-lateral cell membrane (Figure 1e–n, highlighted by arrowheads). Murine hearts[23–28] (Supplementary Figure S3A–I) and skin[8,9,28,29] (Supplementary Figure S3a′–i′) were used as positive controls to confirm the specificity of the antibody staining, and nonspecific IgG (Supplementary Figure S3j and j′) was used as a negative control.

Regulation of Dsg2 in kidney diseases

We next analyzed the regulation of the desmosomal components during disease in the publicly available datasets in the Gene Expression Omnibus database using the Geo2R tool. Compared with healthy mice, an upregulation of several desmosomal genes, especially *Dsg2,* was detected in different kidney disease models (Supplementary Figure S4). Then we reanalyzed our published scRNA-seq datasets from human kidneys for the expression of desmosomal components in TECs.[22] We observed an upregulation of *DSG2* in injured TECs in the kidneys of patients with chronic kidney disease compared with healthy controls (Supplementary Figure S5). In a time course of the murine UUO model[16] (Supplementary Figure S6), we found a significant upregulation of Dsg2 by immunohistochemistry (Figure 2a–g), Western blot (Figure 2h and i), and reverse transcription–quantitative real-time polymerase chain reaction (Figure 2j). Morphologically, in disease, Dsg2 expression was localized along the entire lateral membrane, suggesting aberrant localization outside of the apical-junctional complexes. In addition, *in vitro* studies with the human TEC line HK-2 showed significantly increased Dsg2 expression after challenge with tumor necrosis factor-α (TNF-α) (Figure 2l and m) and particularly with interferon-γ (IFN-γ) (Figure 2n and o). The expression of other desmosomal components, that is, Dsp, Dsg1, and Pg, was also significantly increased after UUO (Supplementary Figure S7).

We next analyzed 3 additional murine models with different types of kidney injury: (i) Alport mice, a transgenic model with *Col4* gene mutation leading to glomerulopathy with secondary tubular injury, mimicking the human Alport syndrome; (ii) I/R injury as a model of acute tubular injury; and (iii) the 2,8-dihydroxyadenine nephropathy modeling crystal-induced TEC injury. Compared with healthy kidneys, the analyzed desmosomal components, including Dsc1, Dsc2, Dsc3, Dsg1, Dsg2, Pkp2, Pkp3, Dsp, and Pg, were all upregulated in these models, particularly in the diseased dilated tubules (Supplementary Figure S8).

Co-stainings with tubular segment–specific markers, such as CD13 and DBA (*Dolichos biflorus* agglutinin), and scRNA-seq data demonstrated that Dsg2 was mainly expressed by collecting ducts, distal tubules, and the descending thin and thick ascending limb, and only weakly detectable in proximal tubular cells (Supplementary Figure S9) but strongly expressed in injured tubules (Supplementary Figure S9C–G). We have analyzed the amount of Dsg2 using immunohistochemistry in human kidney biopsies and resection specimens with various kidney diseases. DSG2 was rarely detected in healthy human kidneys, while it was significantly expressed during various diseases, such as T-cell–mediated rejection, pyelonephritis, autosomal dominant polycystic kidney disease, hydronephrosis/nephrolithiasis, renovascular disease, and acquired cystic kidney disease (Figure 3a–h).

Tubular-specific deletion of *Dsg2* did not affect the expression of other desmosomal proteins and did not result in spontaneous tubular damage

To study the functional role of Dsg2, we have established a genetic mouse model with kidney TEC-specific deletion of *Dsg2* under the Pax8 promoter, the constitutive $Pax8^{Cre/+}::Dsg2^{flox/flox}$ mouse (Cre/+) (Supplementary Figure S10A). The successful deletion of *Dsg2* was verified by immunofluorescence staining (Supplementary Figure S10B–G) and Western blot analysis (Supplementary Figure S10H). Although desmosomal components were described to be expressed in embryonic kidneys,[19] mice with TEC-specific *Dsg2* deletion developed normally without an obvious spontaneous phenotype (Supplementary Figure S10I–L). Kidney expression of other desmosomal components, such as Dsp and Dsg1, did not change in TEC-specific *Dsg2* knockout mice (Supplementary Figure S10M–O). Kidney function was not altered, and also other organs, such as heart, intestine, liver, lung, skin, spleen, or tongue, showed no obvious pathologic abnormalities (Supplementary Figure S11).

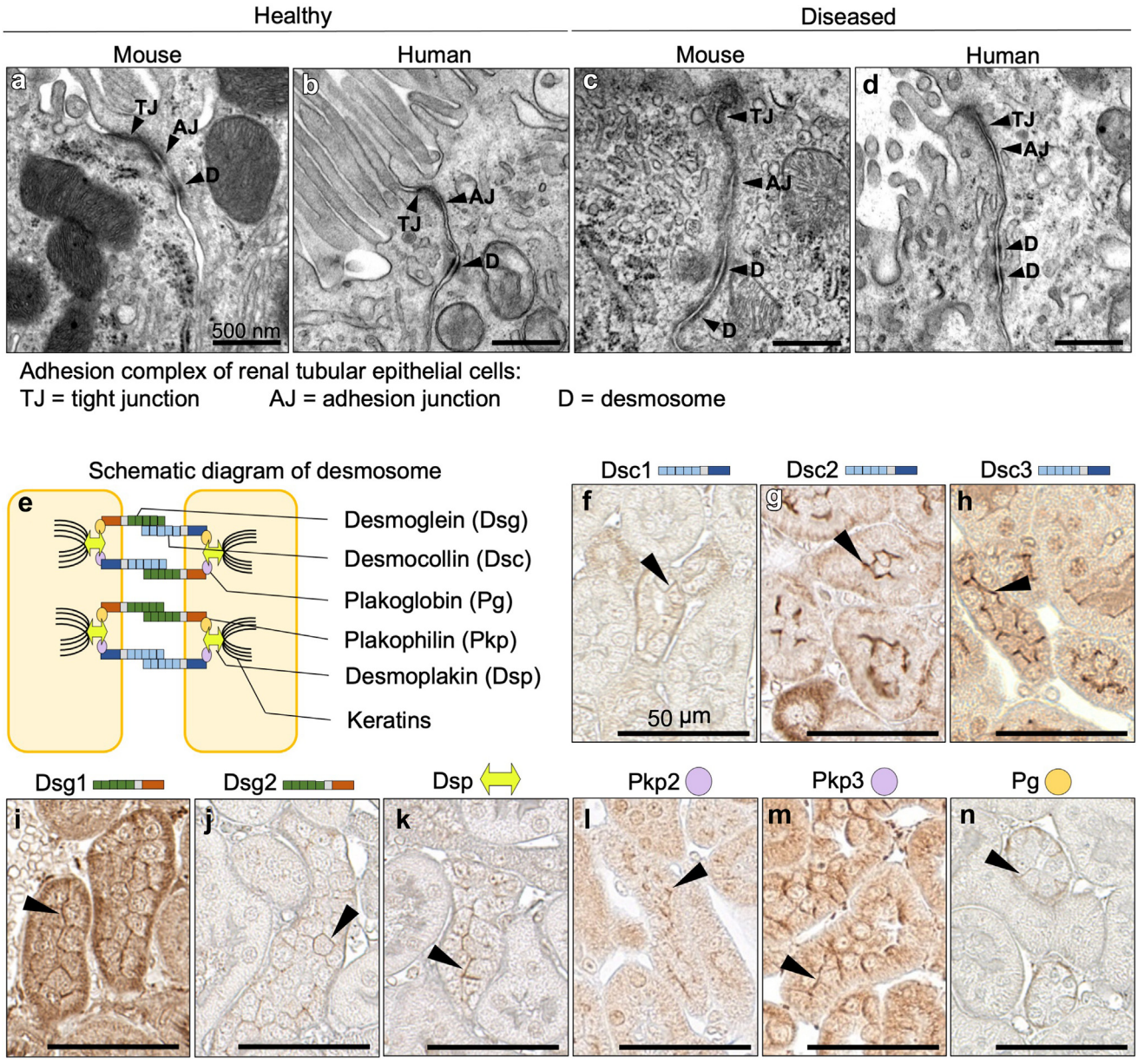

Figure 1 | Desmosomal proteins were detected in healthy kidneys at the apico-junctional complex (AJC). Visualization of cell-cell junctions (**a–d**) by electron microscopy, including tight junction (TJ), adherens junction (AJ), and desmosome (D), in murine and human kidney tubular epithelial cells in healthy and diseased subjects. Bars = 500 nm. (**e**) Schematic diagram of the desmosome structure in tubular epithelial cells. (**f–n**) Desmocollin (Dsc), desmoglein (Dsg), plakoglobin (Pg), plakophilin (Pkp), and desmoplakin (Dsp) were visualized by immunohistochemistry in healthy murine tubular epithelial cells. The arrowheads indicate the location of the respective desmosomal component. Bars = 50 µm. To optimize viewing of this image, please see the online version of this article at www.kidney-international.org.

In the 2,8-dihydroxyadenine nephropathy model, the kidney function showed no differences after knockout *Dsg2* (Supplementary Figure S12). These data suggested that Dsg2 is dispensable for normal kidney development and physiological functions.

Tubular-specific deletion of *Dsg2* increased tubular injury and atrophy in disease models

The establishment of kidney disease animal models is conducive to the study of the relationship between the pathogenesis of kidney disease, changes in tissue morphology, ecological indicators, and clinical manifestations. To understand the role of Dsg2 in kidney disease pathophysiology, we challenged $Pax8^{Cre/+}$::$Dsg2^{flox/flox}$ mice and wild-type littermates with 3 well-established kidney injury models: UUO, I/R, and 2,8-dihydroxyadenine nephropathy.

Our data showed that after 5 days of UUO (Figure 4a), $Ki67^{+}$ TECs significantly increased up to 1.4-fold (Figure 4b–b″) and the number of cleaved $caspase3^{+}$ TECs (Figure 4c–c″) up to 1.6-fold in TEC-specific *Dsg2* knockout mice compared with their wild-type littermates. The number of $Er\text{-}Hr3^{+}$ infiltrating immune cells also significantly increased in

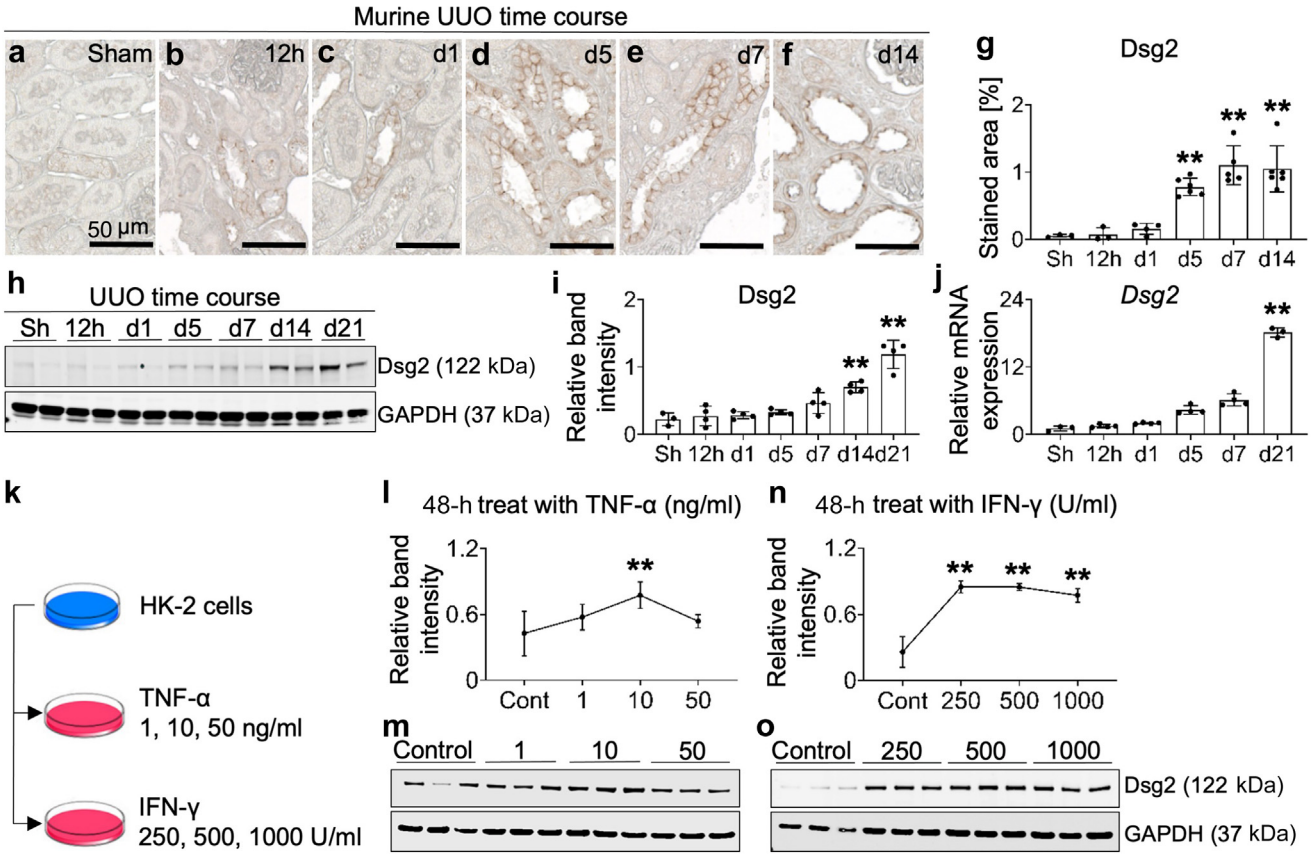

Figure 2 | Expression of desmoglein-2 (Dsg2) was upregulated during stress *in vivo* and *in vitro*. Dsg2 in the murine unilateral ureteral obstruction (UUO) model was significantly increased at the protein level analyzed by (**a–g**) immunohistochemistry staining and (**h,i**) immunoblotting and (**j**) at the RNA level as shown by reverse transcription–quantitative real-time polymerase chain reaction. Bars = 50 µm. (**k**) HK-2 cells were treated for 48 hours with different concentrations of tumor necrosis factor-α (TNF-α) and interferon-γ (IFN-γ); (**l–o**) immunoblotting with morphometric quantification revealed a significant increase in Dsg2 expression. $^{**}P < 0.01$. GAPDH, glyceraldehyde-3-phosphate dehydrogenase; treat, treatment. To optimize viewing of this image, please see the online version of this article at www.kidney-international.org.

Pax8$^{Cre/+}$*::Dsg2*$^{flox/flox}$ mice (Figure 4d–d″). The expression of the tubular injury marker Ngal did not differ between both groups (Figure 4e–e″). In a more advanced disease stage after 10 days of UUO (Figure 4f), transgenic mice lacking tubular *Dsg2* showed a significant increase in Ki67^{+} (Figure 4g–g″) and cleaved caspase3^{+} TECs (Figure 4h–h″), as well as an increase in infiltrating Er-Hr3^{+} immune cells (Figure 4i–i″). Further, a 2-fold increase in Ngal^{+} stained area (Figure 4j–j″) was detectable. Numerically, the increase was more prominent after 10 days than after 5 days of UUO. The total number of tubules (Supplementary Figure S13A), the total number of TECs (Supplementary Figure S13B), and their ratio (Supplementary Figure S13C) were similar between the groups. Normalization of the number of proliferating (Supplementary Figure S13D and E) and apoptotic tubular cells (Supplementary Figure S13F and G) to the total number of tubules (Supplementary Figure S13D and F) or the total number of TECs (Supplementary Figure S13E and G) confirmed the increase due to Dsg2 deficiency. Consistent with the UUO findings, in unilateral I/R injury (day 21) and 2,8-dihydroxyadenine nephropathy (day 14), the transgenic mice showed increased TEC proliferation, apoptosis, and injury, as well as more inflammatory infiltrates (Figure 5). In the 2,8-dihydroxyadenine nephropathy model, but not in the unilateral I/R model, Er-Hr3^{+} cells and Ngal^{+} stained area were significantly increased (Figure 5).

We investigated the effects of *Dsg2* tubular deficiency in acute kidney injury in the bilateral I/R model after 24 hours, allowing also the analysis of kidney function. At this early stage, tubular cell injury and cell death were already significantly increased in *Pax8*$^{Cre/+}$*::Dsg2*$^{flox/flox}$ mice, but in contrast to later stages, TEC proliferation was significantly decreased (Figure 6). To further explore the effects of a Dsg2 deletion in TECs, we measured the area of tubules in the cortical region with a deep learning–based histopathologic assessment. Our data showed that in the UUO model, compared with the control group, more tubules in the transgenic mice were atrophic. This was more prominent at the later stage of the model at day 10 (Figure 7). The tubular-specific deletion of *Dsg2* increased tubular cell loss at UUO day 10 analyzed by counting the tubules containing cell debris in the tubular lumen (Figure 7d–d″) and the adenine model by analyzing

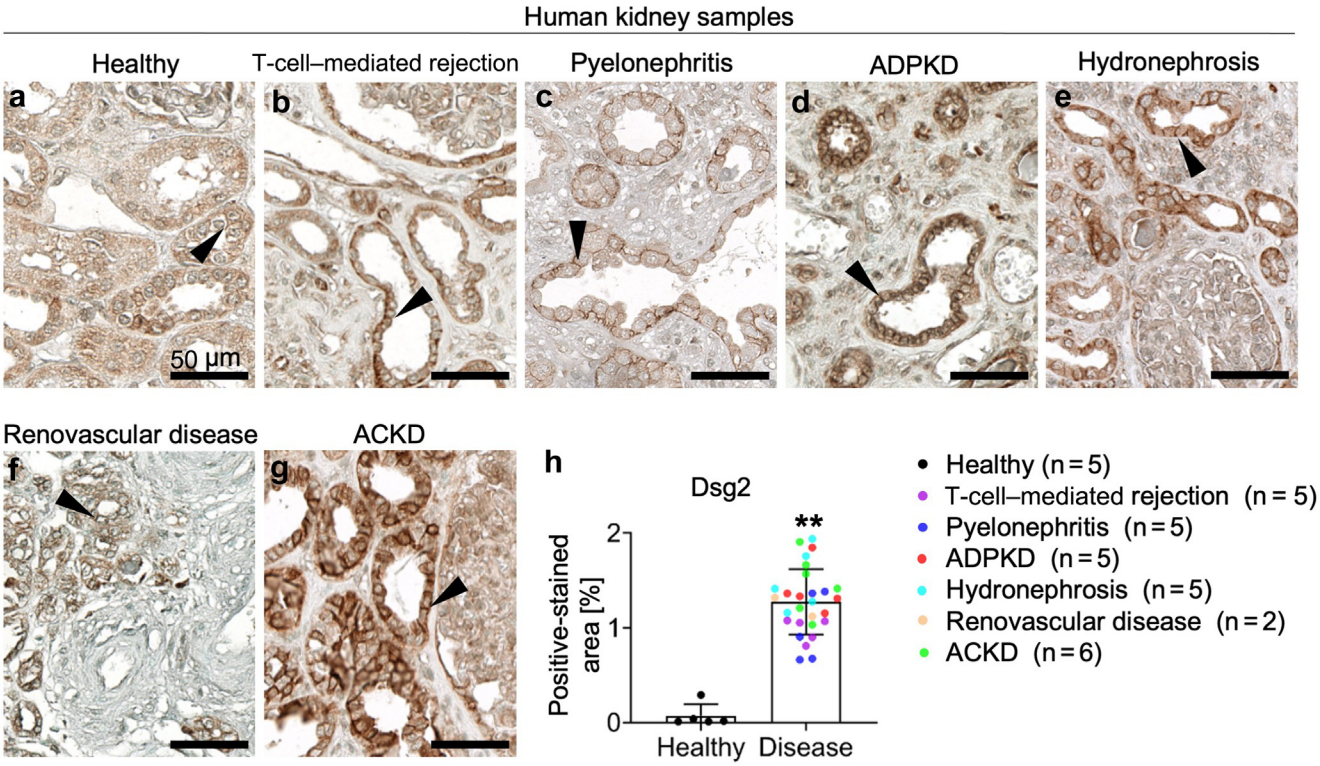

Figure 3 | Expression of desmoglein-2 (DSG2) was upregulated in different human kidney diseases. (**a**) A significant increase in different human kidney diseases compared with healthy controls, where the arrowheads indicate the location of DSG2 in (**b**) T-cell–mediated rejection, (**c**) pyelonephritis, (**d**) autosomal dominant polycystic kidney disease (ADPKD), (**e**) hydronephrosis due to nephrolithiasis, (**f**) renovascular disease, and (**g**) acquired cystic kidney disease (ACKD), shown by (**h**) the quantification of the DSG2-positive stained area in human kidney cortex. Bars = 50 µm. $^{**}P < 0.01$. To optimize viewing of this image, please see the online version of this article at www.kidney-international.org.

the urine for keratin 18 and its caspase-cleaved fragment (Figure 7e–g).

Immunofluorescence staining of tubular segments with specific markers, such as CD13 for proximal tubules and Tamm-Horsfall protein (THP) for distal tubules, revealed that the cell debris in the tubular lumen of the Dsg2-deficient mice were THP+ (Supplementary Figure S14A–A″). Reanalysis of TEC proliferation in these 2 different tubular segments showed that the increase in TEC proliferation is also mainly in THP+ (Supplementary Figure S14B–E) and not in CD13+ TECs (Supplementary Figure S14F–I).

Next, we investigated the expression of 118 different cytokines in kidneys of *Pax8Cre::Dsg2*$^{flox/flox}$ mice compared with wild-type littermates after 14 days of adenine-enriched diet. Twenty-one proteins were differentially regulated in the Dsg2-deficient mice, 19 up- and 2 downregulated. These included tubular injury markers Kim-1 and Ngal or proinflammatory cytokines TNF-α and IFN-γ (Figure 7h).

Lack of *DSG2*-weakened cell connections in HK-2 cells *in vitro*

Using the human TEC line HK-2, we suppressed *DSG2* gene expression *via* small, interfering RNA and confirmed the successful downregulation by Western blot analysis and immunofluorescence staining (Supplementary Figure S15A–D).

To study the role of Dsg2 in cell adhesion, we treated the confluent cell monolayer with dispase to release it from the bottom of cell culture flasks. This monolayer was then subjected to shear stress by pipetting. Shear stress resulted in an increased number of small fragments of the original monolayer. This fragmentation was more pronounced in small, interfering RNA-*DSG2*–treated cells compared with the controls (Figure 8a–g), suggesting a weakening of cell-cell adhesion following reduced Dsg2 expression. To analyze the effect of *DSG2* deficiency on cell proliferation and cell death, HK-2 cells were transfected with small, interfering RNA-*DSG2* or the control small, interfering RNA-NT and challenged with 15% fetal calf serum to induce proliferation or with IFN-γ or TNF-α to induce cell stress/death. *DSG2* deficiency led to a transient reduction of cell proliferation in a mitogenic setting (fetal calf serum stimulation, Figure 8h), but to an increased proliferation under stress (induced by IFN-γ [Figure 8i] or TNF-α [Figure 8j]). In parallel, cell death was significantly higher in tubular cells lacking *DSG2* (Figure 8h′–j′).

DISCUSSION

Our study is the first to comprehensively analyze the expression and regulation of desmosomal components and the functional role of Dsg2 in kidney TECs *in vivo*. Our data are in line with the previous 3 reports describing the expression of Dsg1,[18,19] Dsg2,[17] Dsc2/3,[18,19] Dsp,[17–19], and Pg[17] in TECs.

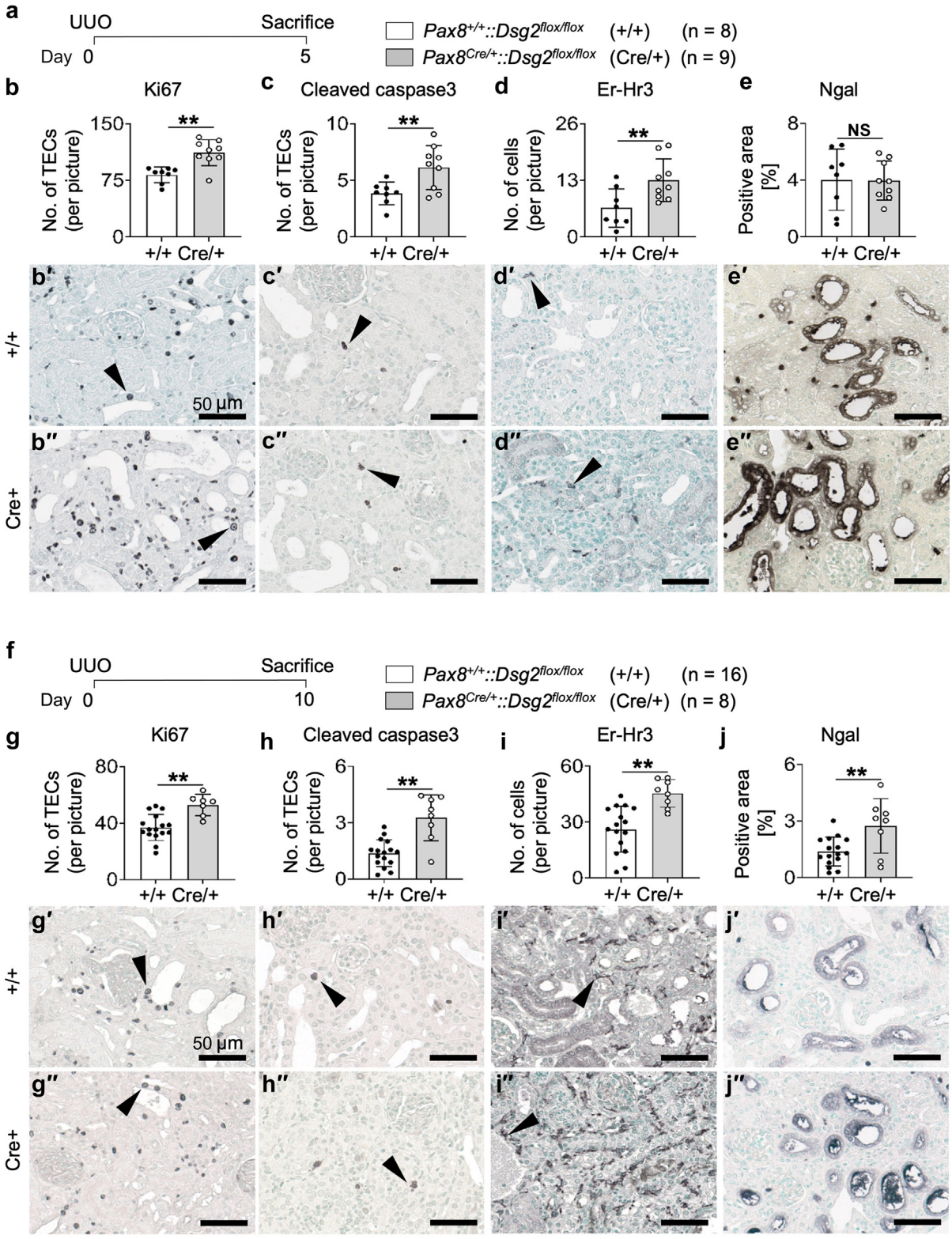

Figure 4 | Tubular cell–specific *Dsg2* deficiency induced tubular injury and inflammation in the unilateral ureteral obstruction (UUO) model in mice. (**a**) After 5 days of UUO, mice lacking *Dsg2* (Cre/+) in tubular cells showed a significant increase in (**b–b″**) Ki67$^+$ and (**c–c″**) cleaved caspase3$^+$ tubular epithelial cells (TECs) and the amount of (**d–d″**) ErHr3$^+$ immune cells compared with wild-type littermates (+/+) (shown with arrowheads), whereas the percentage of (**e–e″**) Ngal$^+$-stained area has not changed. At day 10 after (**f**) UUO, Cre/+ mice showed a significant increase in (**g–g″**) Ki67$^+$ and (**h–h″**) cleaved caspase3$^+$ TECs. In addition, (**i–i″**) more ErHr3$^+$ immune cells were seen (as shown by arrowheads), and (**j–j″**) a stronger tubular injury, analyzed by the Ngal$^+$-stained area, was detectable. Bars = 50 µm. $^{**}P < 0.01$. Dsg2, desmoglein-2; NS, not significant. To optimize viewing of this image, please see the online version of this article at www.kidney-international.org.

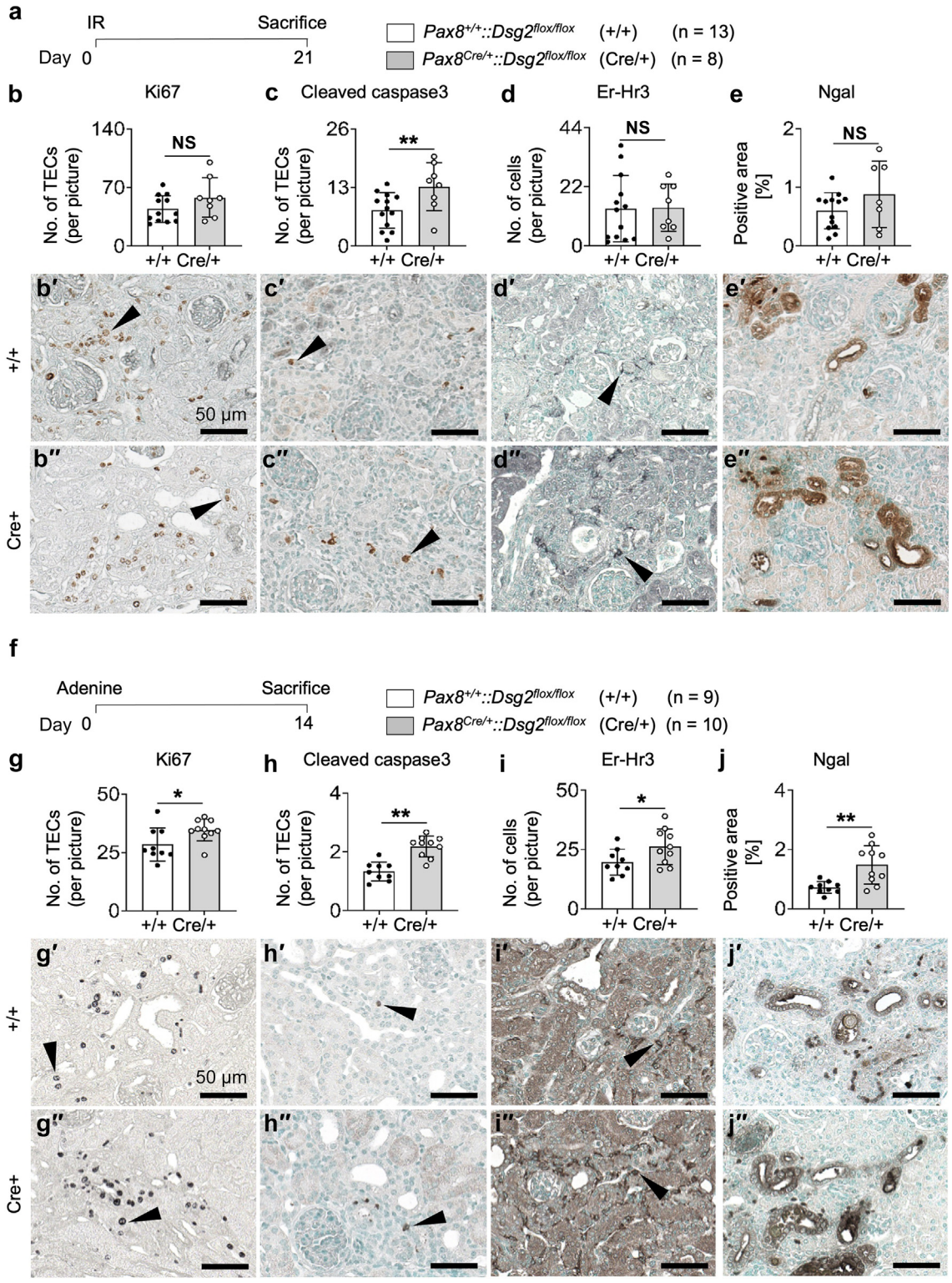

Figure 5 | Tubular cell–specific *Dsg2* deficiency intensified tubular injury and inflammation in ischemia-reperfusion (I/R) and 2,8-dihydroxyadenine nephropathy model in mice. In the model of unilateral ischemia reperfusion at (**a**) day 21 (I/R), the tubular epithelial cell (TEC)–specific *Dsg2* knockout mice (Cre/+) showed a significant increase in (**c**) cleaved caspase3$^+$ expression in TECs (arrowheads), whereas no difference was detectable in the amount of (**b**) Ki67 positive TECs, (**d**) Er-Hr3$^+$ immune cells (as shown by arrowheads), or (**e**) the Ngal positive area in comparison with wild-type littermates (+/+). Fourteen days after (**f**) 2,8-dihydroxyadenine nephropathy (adenine), the Cre/+ mice showed a significant increase in (**g**) Ki67$^+$ and (**h**) cleaved caspase3$^+$ TECs (arrowheads). In addition, the tubular-specific deletion led to an increase in (**i**) the Er-Hr3$^+$ immune cell infiltration (shown by arrowheads) and in tubular injury, visualized by (**j**) Ngal staining. Bars = 50 µm. *$P < 0.05$, **$P < 0.01$. Dsg2, desmoglein-2; NS, not significant. To optimize viewing of this image, please see the online version of this article at www.kidney-international.org.

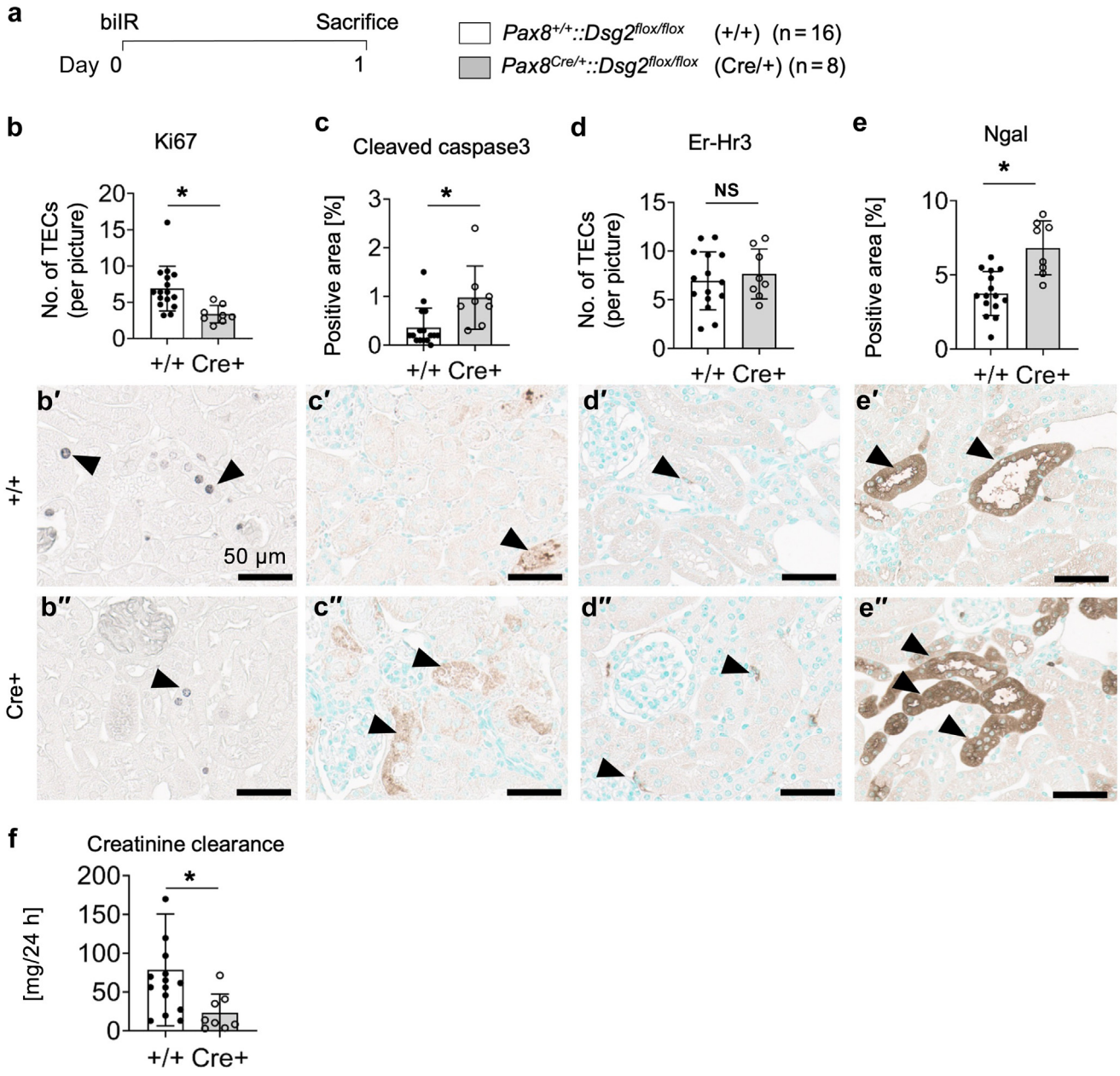

Figure 6 | Tubular cell–specific *Dsg2* deficiency in early acute kidney injury (AKI) increased tubular cell injury and tubular cell death. AKI was induced by (**a**) bilateral ischemia-reperfusion (bilR) for 24 hours. Mice lacking *Dsg2* (Cre/+) in tubular cells showed (**b–b″**) a significant decrease in Ki67^{+} and (**c–c″**) an increase in cleaved caspase3^{+} tubular epithelial cells (TECs). The amount of (**d–d″**) ErHr3+ immune cells compared with wild-type littermates (+/+) (shown with arrowheads) has not changed, whereas the percentage of (**e–e″**) Ngal^{+} area increased. (**f**) Creatinine clearance was significantly reduced in *Dsg2*-deficient mice. *$P < 0.05$. Dsg2, desmoglein-2; NS, not significant. To optimize viewing of this image, please see the online version of this article at www.kidney-international.org.

The kidney tubular cell–specific *Dsg2* knockout in mice showed no obvious spontaneous pathologic phenotype and no changes in kidney function. This is in line with our previous study, showing that Dsg2 was not required for desmosomal assembly and embryonic development in the intestine.[30] Conversely, *Dsg2* knockout in the intestine enhanced intestinal epithelial barrier disruption after challenging the mice with dextran sodium sulfate,[30] and *Dsg2* knockout in cardiomyocytes led to the development of arrhythmogenic cardiomyopathy.[23–28] This suggests that Dsg2 is essential for the desmosomal function of tissues subjected to intense mechanical stress under physiological conditions like the heart but is dispensable in the kidneys. In healthy kidney TECs, we found a low basal expression of desmosomal proteins. This is in line with studies showing low amounts of Dsg2 and Dsc2 expression in healthy mouse kidneys[30] and weak Dsg1/2 in healthy human kidneys.[18] We observed increased expression of the majority of desmosomal proteins during kidney disease *in vivo* in both mice and patients, including Dsg2. This increase was particularly localized to

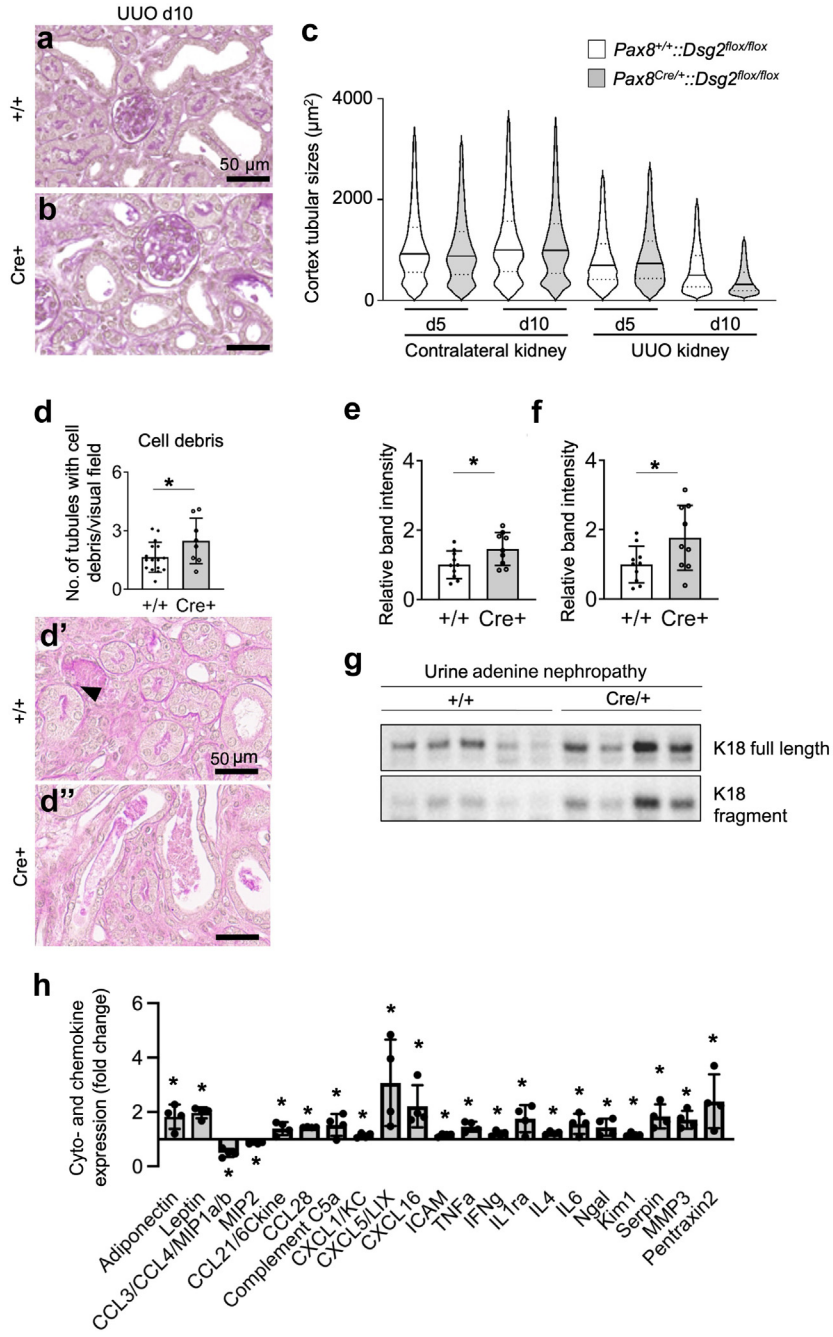

Figure 7 | Tubular cell–specific *Dsg2* deficiency induced tubular atrophy and tubular cell loss. (**a**) Periodic acid–Schiff staining of kidneys from wild-type littermates (+/+) and (**b**) mice with tubular cell–specific deletion of *Dsg2* (cre/+) 10 days after unilateral ureteral obstruction (UUO). (**c**) Compared with wild-type littermates, the size of tubules in *Dsg2*-deficient mice showed no major difference between the contralateral control and the UUO-subjected kidney at day 5 group, whereas a stronger decrease in the tubular size was observed in the *Dsg2*-deficient mice at UUO day 10, hinting to more tubular atrophy. At UUO day 10, (**d**) the number of tubules containing cell debris per visual field was counted in (**d′**) wild-type littermates and (**d″**) mice with tubular cell–specific deletion of *Dsg2*. (**e**) Urine analysis of full-length keratin 18 (K18) or (**f**) caspase-cleaved K18 fragment by (**g**) Western blot revealed an increase in tubular cell loss in *Dsg2*-deficient mice fed for 14 days an adenine-enriched diet. (**h**) Cytokine and chemokine array analysis of tissue lysats from *Dsg2*-deficient mice compared with wild-type littermates showed 21 differentially expressed proteins. Bars = 50 µm; *$P > 0.05$. CCL, CC chemokine ligand; CXCL, CXC chemokine ligand; Dsg2, desmoglein-2; ICAM, intercellular adhesion molecule; IFN, interferon; IL, interleukin; MMP, matrix metalloproteinase; TNF-α, tumor necrosis factor-α. To optimize viewing of this image, please see the online version of this article at www.kidney-international.org.

dilated tubules. A previous study showed that the mechanical tension on TECs was increased during UUO.[31,32] Our data suggest that the increased expression of desmosomal proteins might be the response to mechanical stress. Our data showed that Dsg2 is mostly expressed outside the proximal tubular compartment, particularly in the distal tubules and collecting

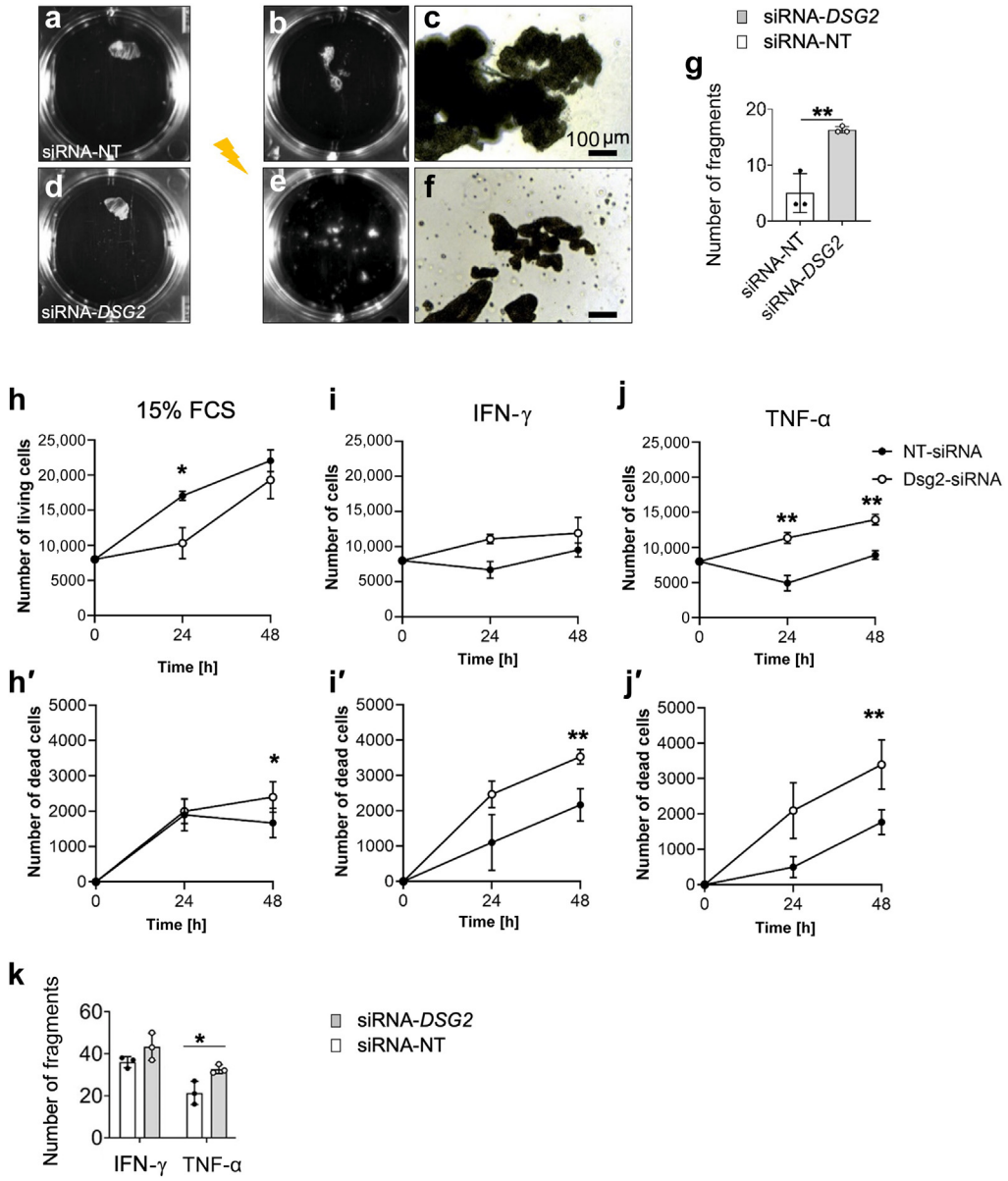

Figure 8 | *DSG2* knockout promoted proliferation and reduced cell-cell adhesion in HK-2 cells *in vitro*. The dispase-based dissociation assay was used to evaluate the strength of cell-cell adhesion. HK-2 cell sheets (**a**) with or (**d**) without DSG2 were released from the cell culture dish and subjected to mechanical force as described in the Supplementary Methods. (**b–f**) Representative images of fragmentation induced by mechanical force. (**g**) The resulting fragments were counted. (**h,h′**) HK-2 cells with and without *DSG2* were stimulated with 15% fetal calf serum (FCS), (**i,i′**) interferon-γ (IFN-γ), or (**j,j′**) tumor necrosis factor-α (TNF-α), and (**h–j**) the number of living and (**h′–j′**) dead cells was counted. (**k**) Under proinflammatory conditions, the effect of *DSG2* deficiency on cell-cell adhesion was analyzed with the dispase-based dissociation assay. Bars = 100 µm. *$P < 0.05$, **$P < 0.01$. Dsg2, desmoglein-2; siRNA, small, interfering RNA. To optimize viewing of this image, please see the online version of this article at www.kidney-international.org.

ducts. Proximal tubular cells are usually considered the important cells driving kidney disease inflammation and progression in the models analyzed. Therefore, our data suggest that the distal tubular compartment might also be important in driving the progression of the reported models, in line with some previous reports.[33–38] Our data indicate that due to Dsg2 deficiency, there is an increased cell loss and thus more regeneration/proliferation, especially in the tubular segment where Dsg2 is mainly expressed, namely the distal THP+ tubules.

In the various diseases, we observed the expression of Dsg2 and other desmosomal proteins along the whole lateral membrane of TECs. Desmosomes are normally located at the apical-junctional complex in TECs,[4] and we also have not observed desmosomal structures in electron microscopy outside of apical-junctional complexes, neither in healthy nor diseased TECs. This might suggest an extradesmosomal location of Dsg2. Similar findings were described in other desmosome-rich tissues, such as cell membranes of epithelia, which were strongly Dsg2-positive in the healthy intestine,[30]

endometrium,[39] and skin.[40] One study suggested that an extradesmosomal Dsg2 on the surface of polarized enterocytes regulated intestinal barrier function *via* mitogen-activated protein kinase (p38MAPK) signaling *in vitro* [41]. The extradesmosomal Dsg3 was detected in keratinocytes *in vitro*, and this extradesmosomal Dsg3 could form a signaling complex together with E-cadherin, β-catenin, and Rous sarcoma kinase to strengthen keratinocyte cohesion also *via* p38MAPK signaling.[29,42] The exact role of extradesmosomal Dsg2 in the kidney remains unclear and will require future studies.

In our transgenic mice, we did not observe any changes in other members of the desmosome such as Dsg1 or Dsp, which could potentially compensate for the lack of Dsg2. Together with our findings of the functional consequences of Dsg2 deletion in TECs, this supports the hypothesis that other desmosomal components are not able to compensate for the loss of one specific desmosomal protein.[28]

In the examined disease models, *Dsg2* deletion led to several changes in TECs. The observed increased TEC apoptosis *in vivo and in vitro* was similar to previous studies showing cardiomyocyte apoptosis as an early finding in Dsg2-related heart disease.[10] Also, we previously found a higher level of cleaved caspase-1 in the intestine in mice lacking *Dsg2*,[30] and the absence of other components of desmosomes in the skin, such as Dsg1 and Dsg3, caused increased apoptosis *in vivo*.[11] Previous studies showed that abnormal connections between neighboring epithelial cells or between cells and matrix might lead to an increase in cell death,[43] and the integrity of desmosomes is essential for extruding apoptotic cells and maintaining tissue stability *in vitro*.[44] For intestinal epithelial cells, it was shown that for cell survival, cell-cell or cell-matrix adhesion is required and that loss of such cell adhesion induced epithelial cell death in part by apoptosis.[45] This is supported by upregulation of chemokines, including CC chemokine ligand 28, C5a, CXC chemokine ligand 16, and KC (CXC chemokine ligand 1), which induce apoptosis. Our *in vivo* and *in vitro* data suggest a similar mechanism for renal TECs. Although our *in vitro* data were in line with the *in vivo* findings, a limitation of our study is that we only used the HK-2 cell line and not primary tubular cells. Increased regeneration/proliferation of TECs was another alteration we observed in TECs lacking *Dsg2* during disease *in vivo*. Similar changes were seen in intestinal epithelial cell–specific Dsg2 knockout mice.[30] Currently, the different effects of *Dsg2* deficiency on tubular cell proliferation in early versus late disease stages *in vivo* and proliferative versus stress stimulation *in vitro*, and the interplay with apoptosis, remain unclear. Possibly, the different extent and importance of cell death versus regeneration during the disease stages might play a role. Lastly, we observed an increased inflammatory cell infiltration in $Pax8^{Cre/+}::Dsg2^{flox/flox}$ mice during kidney disease. This is in line with a previous study in the intestine showing that lack of *Dsg2* caused a strong inflammatory response due to the activation of proinflammatory cytokines interleukin-1β/TNF-α and interleukin-22–phosphorylated signal transducer[41] and activator of transcription 3 signaling.[30]

We were not able to pinpoint the connection between the different effects of Dsg2 deficiency on tubular cell proliferation in early versus late disease stages *in vivo* and proliferative versus stress stimulation *in vitro*, and the interplay with apoptosis. We have analyzed the previously proposed signaling pathways, particularly the MAPK (analyzing p38 and extracellular signal–regulated kinase phosphorylation), epidermal growth factor receptor, and signal transducer and activator of transcription 3 pathways. However, none of these pathways were significantly affected in the kidney tissues, suggesting that they might not be involved (data not shown). A limitation of these analyses might be that they were performed in full kidney samples so that changes in the (distal) tubular compartment could have been masked. In summary, our findings suggest that desmosomes, particularly Dsg2, are dispensable for embryonic development and physiological kidney function but are upregulated in various diseases in mice and patients and protect tubular cells from injury in different models of kidney diseases.

DISCLOSURE

All the authors declared no competing interests.

DATA STATEMENT

All animal studies were performed and the data generated at the University Hospital Aachen. All data are available in the main text or the Supplementary Material. This article does not report original code. Any additional information required to reanalyze the data reported in this paper is available from the lead contact upon request. The datasets analyzed in this study are available from the Gene Expression Omnibus repository under the following accession numbers: GSE96101, GSE85409, GSE32583, GSE52004, GSE87023, GSE7869, GSE66494, GSE30718, and GSE32591. The human data were approved by the local review board of the University Hospital RWTH Aachen (EK244/14, EK042/17, and EK016/17) and are available under restricted access for legal and privacy protection reasons; access can be obtained by contacting Peter Boor, Institute of Pathology, RWTH Aachen University Clinic, Aachen, Germany (pboor@ukaachen.de). In general, the requests will be processed based on institutional and national policies. Data can only be shared for noncommercial research purposes and require a data transfer agreement that is provided by the legal department of the University Hospital RWTH Aachen. The detailed protocol of scRNA-seq was described in a previous publication (https://doi.org/10.1038/s41586-020-2941-1).

ACKNOWLEDGMENTS

We thank Simon Otten, Christina Gianussis, Louisa Böttcher, Jana Baues, and Marie Cherelle Timm for their technical support.

FUNDING STATEMENT

The study was supported by the German Research Foundation (DFG, Project IDs 322900939 and 454024652 to PB, 432698239 to PB and SD, and 445703531 to PB, SD, and BMK), European Research Council (ERC Consolidator Grant No. 101001791 to PB), and the Federal Ministry of Education and Research (BMBF, STOP-FSGS-01GM1901A to PB and SD). PS is supported by the DFG (STR1095/6-1).

SUPPLEMENTARY MATERIAL

Supplementary File (PDF)

Supplementary Methods. *In vitro* cell culture and siRNA transfection; histology, immunohistochemistry, and immunofluorescence; RNA extraction and analysis; Western blot analysis; dispase-based dissociation array; proliferation and cell death analysis; reanalysis of public arrays; digital data analysis; and single-cell RNA sequencing.

Supplementary Figure S1. Patient characteristics.

Supplementary Figure S2. The expression of mRNA of desmosomal components in human kidneys analyzed using scRNA sequencing.

Supplementary Figure S3. The expression of desmosomal proteins in heart and skin used as positive controls for the immunohistochemistry studies.

Supplementary Figure S4. The expression of desmosomal mRNA in animal models by reanalysis of publicly available datasets.

Supplementary Figure S5. The expression of desmosomal mRNA in human injured kidney tubules analyzed using single-cell RNA sequencing.

Supplementary Figure S6. Histologic assessment of UUO confirmed expected tubular injury pattern.

Supplementary Figure S7. Regulation of desmosomal components in the UUO model.

Supplementary Figure S8. The expression of desmosomal proteins in I/R, Alport, and Adenine murine models.

Supplementary Figure S9. Dsg2 is predominately expressed in distal tubules and collecting ducts.

Supplementary Figure S10. Confirmation of *Dsg2* knockout and retained composition of desmosomal components in the transgenic mice *in vivo*.

Supplementary Figure S11. Tubular-specific knockout of Dsg2 has no influence on kidney function or other organ development.

Supplementary Figure S12. Dsg2 deletion did not affect kidney function in the adenine model.

Supplementary Figure S13. Normalization of proliferation and apoptosis to the total number of tubules and tubular epithelial cells confirmed an increase due to tubular-specific Dsg2 deficiency in the UUO model.

Supplementary Figure S14. Tubular cell–specific Dsg2 deficiency–induced cell loss and proliferation in distal tubules.

Supplementary Figure S15. Confirmation of *Dsg2* knockout in HK-2 cells *in vitro*.

Supplementary Table S1. Incubation times and cytokine concentrations.

Supplementary Table S2. Primary antibodies list.

Supplementary Table S3. Secondary antibodies used for immunohistochemistry.

Supplementary Table S4. Bokemeyer buffer.

Supplementary Table S5. Secondary antibodies used for Western blot.

Supplementary Table S6. List of analyzed publicly available datasets.

Supplementary References.

REFERENCES

1. Grgic I, Campanholle G, Bijol V, et al. Targeted proximal tubule injury triggers interstitial fibrosis and glomerulosclerosis. *Kidney Int*. 2012;82:172–183.
2. Saito M, Tucker DK, Kohlhorst D, et al. Classical and desmosomal cadherins at a glance. *J Cell Sci*. 2012;125:2547–2552.
3. Windoffer R, Borchert-Stuhlträger M, Leube RE. Desmosomes: interconnected calcium-dependent structures of remarkable stability with significant integral membrane protein turnover. *J Cell Sci*. 2002;115:1717–1732.
4. Delva E, Tucker DK, Kowalczyk AP. The desmosome. *Cold Spring Harb Perspect Biol*. 2009;1:a002543.
5. Nie Z, Merritt A, Rouhi-Parkouhi M, et al. Membrane-impermeable cross-linking provides evidence for homophilic, isoform-specific binding of desmosomal cadherins in epithelial cells. *J Biol Chem*. 2011;286:2143–2154.
6. Hatzfeld M. Plakophilins: multifunctional proteins or just regulators of desmosomal adhesion? *Biochim Biophys Acta*. 2007;1773:69–77.
7. Bass-Zubek AE, Godsel LM, Delmar M, Green KJ. Plakophilins: multifunctional scaffolds for adhesion and signaling. *Curr Opin Cell Biol*. 2009;21:708–716.
8. Spindler V, Waschke J. Pemphigus—a disease of desmosome dysfunction caused by multiple mechanisms. *Front Immunol*. 2018;9:136.
9. Vielmuth F, Walter E, Fuchs M, et al. Keratins regulate p38MAPK-dependent desmoglein binding properties in pemphigus. *Front Immunol*. 2018;9:528.
10. Ng K-E, Delaney PJ, Thenet D, et al. Early cardiac inflammation as a driver of murine model of Arrhythmogenic Cardiomyopathy. Preprint. bioRxiv. 169664. Posted online June 26, 2020. https://10.1101/2020.06.24.169664
11. Schmidt E, Waschke J. Apoptosis in pemphigus. *Autoimmun Rev*. 2009;8:533–537.
12. Kamekura R, Kolegraff K, Nava P, et al. Loss of the desmosomal cadherin desmoglein-2 suppresses colon cancer cell proliferation through EGFR signaling. *Oncogene*. 2014;33:4531–4536.
13. Overmiller AM, McGuinn KP, Roberts BJ, et al. c-Src/Cav1-dependent activation of the EGFR by Dsg2. *Oncotarget*. 2016;7:37536.
14. Pilichou K, Thiene G, Bauce B, et al. Arrhythmogenic cardiomyopathy. *Orphanet J Rare Dis*. 2016;11:33.
15. Lubos N, van der Gaag S, Gercek M, et al. Inflammation shapes pathogenesis of murine arrhythmogenic cardiomyopathy. *Basic Res Cardiol*. 2020;115:42.
16. Djudjaj S, Papasotiriou M, Bülow RD, et al. Keratins are novel markers of renal epithelial cell injury. *Kidney Int*. 2016;89:792–808.
17. Silberberg M, Charron AJ, Bacallao R, Wandinger-Ness A. Mispolarization of desmosomal proteins and altered intercellular adhesion in autosomal dominant polycystic kidney disease. *Am J Physiol*. 2005;288:F1153–F1163.
18. Russo RJ, Husson H, Joly D, et al. Impaired formation of desmosomal junctions in ADPKD epithelia. *Histochem Cell Biol*. 2005;124:487–497.
19. Garrod D, Fleming S. Early expression of desmosomal components during kidney tubule morphogenesis in human and murine embryos. *Development*. 1990;108:313–321.
20. Buhl EM, Djudjaj S, Babickova J, et al. The role of PDGF-D in healthy and fibrotic kidneys. *Kidney Int*. 2016;89:848–861.
21. Klinkhammer BM, Djudjaj S, Kunter U, et al. Cellular and molecular mechanisms of kidney injury in 2, 8-dihydroxyadenine nephropathy. *J Am Soc Nephrol*. 2020;31:799–816.
22. Kuppe C, Ibrahim MM, Kranz J, et al. Decoding myofibroblast origins in human kidney fibrosis. *Nature*. 2021;589:281–286.
23. Lahtinen AM, Lehtonen E, Marjamaa A, et al. Population-prevalent desmosomal mutations predisposing to arrhythmogenic right ventricular cardiomyopathy. *Heart Rhythm*. 2011;8:1214–1221.
24. Asimaki A, Syrris P, Wichter T, et al. A novel dominant mutation in plakoglobin causes arrhythmogenic right ventricular cardiomyopathy. *Am J Hum Genet*. 2007;81:964–973.
25. Fernandes MP, Azevedo O, Pereira V, et al. Arrhythmogenic right ventricular cardiomyopathy with left ventricular involvement: a novel splice site mutation in the DSG2 gene. *Cardiology*. 2015;130:159–161.
26. Wang L, Liu S, Zhang H, et al. Arrhythmogenic cardiomyopathy: identification of desmosomal gene variations and desmosomal protein expression in variation carriers. *Exp Ther Med*. 2018;15:2255–2262.
27. Kant S, Holthöfer B, Magin TM, et al. Desmoglein 2–dependent arrhythmogenic cardiomyopathy is caused by a loss of adhesive function. *Circ Cardiovasc Genet*. 2015;8:553–563.
28. Najor NA. Desmosomes in human disease. *Annu Rev Pathol*. 2018;13:51–70.
29. Waschke J, Spindler V. Desmosomes and extradesmosomal adhesive signaling contacts in pemphigus. *Med Res Rev*. 2014;34:1127–1145.
30. Gross A, Pack LA, Schacht GM, et al. Desmoglein 2, but not desmocollin 2, protects intestinal epithelia from injury. *Mucosal Immunol*. 2018;11:1630–1639.
31. Rohatgi R, Flores D. Intra-tubular hydrodynamic forces influence tubulo-interstitial fibrosis in the kidney. *Curr Opin Nephrol Hypertens*. 2010;19:65.
32. Quinlan MR, Docherty NG, Watson RWG, Fitzpatrick JM. Exploring mechanisms involved in renal tubular sensing of mechanical stretch following ureteric obstruction. *Am J Physiol Renal Physiol*. 2008;295:F1–F11.
33. Nam SA, Kim WY, Kim JW, et al. Autophagy attenuates tubulointerstital fibrosis through regulating transforming growth factor-β and NLRP3 inflammasome signaling pathway. *Cell Death Dis*. 2019;10:78.

34. Cachat F, Lange-Sperandio B, Chang AY, et al. Ureteral obstruction in neonatal mice elicits segment-specific tubular cell responses leading to nephron loss. *Kidney Int*. 2003;63:564–575.
35. Gao C, Zhang L, Chen EN, et al. Aqp2 progenitor cells maintain and repair distal renal segments. *J Am Soc Nephrol*. 2022;33:1357–1376.
36. Lee SY, Shin JA, Kwon HM, et al. Renal ischemia-reperfusion injury causes intercalated cell-specific disruption of occludin in the collecting duct. *Histochem Cell Biol*. 2011;136:637–647.
37. Denic A, Gaddam M, Moustafa A, et al. Tubular and glomerular size by cortex depth as predictor of progressive CKD after radical nephrectomy for tumor. *J Am Soc Nephrol*. 2023;34:1535–1545.
38. Ren J, Rudemiller NP, Wen Y, et al. The transcription factor Twist1 in the distal nephron but not in macrophages propagates aristolochic acid nephropathy. *Kidney Int*. 2020;97:119–129.
39. Buck VU, Hodecker M, Eisner S, et al. Ultrastructural changes in endometrial desmosomes of desmoglein 2 mutant mice. *Cell Tissue Res*. 2018;374:317–327.
40. Gupta A, Nitoiu D, Brennan-Crispi D, et al. Cell cycle-and cancer-associated gene networks activated by Dsg2: evidence of cystatin A deregulation and a potential role in cell-cell adhesion. *PLoS One*. 2015;10:e0120091.
41. Ungewiß H, Vielmuth F, Suzuki ST, et al. Desmoglein 2 regulates the intestinal epithelial barrier via p38 mitogen-activated protein kinase. *Sci Rep*. 2017;7:6329.
42. Rötzer V, Hartlieb E, Vielmuth F, et al. E-cadherin and Src associate with extradesmosomal Dsg3 and modulate desmosome assembly and adhesion. *Cell Mol Life Sci*. 2015;72:4885–4897.
43. Valentijn A, Zouq N, Gilmore A. *Anoikis. Biochem Soc Trans*. 2004;32:421–425.
44. Thomas M, Ladoux B, Toyama Y. Desmosomal junctions govern tissue integrity and actomyosin contractility in apoptotic cell extrusion. *Curr Biol*. 2020;30:682–690.e685.
45. Nava P, Laukoetter MG, Hopkins AM, et al. Desmoglein-2: a novel regulator of apoptosis in the intestinal epithelium. *Mol Biol Cell*. 2007;18:4565–4578.